

EFFECTS OF MAGNESIUM CONCENTRATION AND LAYER THICKNESS ON THE ADHESION OF PHYSICAL VAPOR DEPOSITED ZNMg-ZN BI-LAYER COATINGS

SOHEIL SABOONI¹, EMAD GALINMOGHADDAM¹, RUUD JOHANNES WESTERWAAL²,
EDZO ZOESTBERGEN² & YUTAO PEI¹

¹Department of Advanced Production Engineering, University of Groningen, The Netherlands

²Tata Steel Nederland Technology, The Netherlands

ABSTRACT

For many years, zinc coatings have been regarded as one of the most effective anti-corrosion protective coatings for steel. Recently, it was shown that the addition of even small amounts of magnesium (Mg) to a zinc (Zn) coating can noticeably increase its corrosion protection performance; however, it has also been observed that there is poor adhesion of zinc-magnesium (ZnMg) coatings to advanced high-strength steels. The addition of a more ductile Zn interlayer between the steel substrate and the ZnMg coating is a solution to improve the adhesion problem. In the present study, a series of ZnMg-Zn bi-layered coatings with different Mg concentrations (up to 14.1 wt.% Mg), and also different thicknesses of the Zn and ZnMg layers, were prepared by a thermal evaporation process (physical vapor deposition (PVD)) in order to investigate the adhesion performance and interfacial adhesion strength. The adhesion performance of these coatings was qualified by the BMW crash adhesion test (BMW AA-M223), while the interfacial adhesion strength at the ZnMg/Zn interface was quantified by the scratch test. It was found that the interfacial adhesion strength decreases gradually with an increase in the Mg content of the top layer. The novel finding is that the interfacial adhesion strength at the ZnMg/Zn interface is independent of the thickness of the Zn interlayer; however, the adhesion performance of a ZnMg-Zn bi-layered coating during a bending test is a complex function of different parameters, such as the thickness of the Zn and ZnMg layers, the interfacial adhesion strength and the interfacial defects density.

Keywords: adhesion strength, bi-layered coating, crash adhesion test, magnesium, physical vapor deposition, scratch test, zinc.

1 INTRODUCTION

For many years, zinc (Zn) coatings have been known as one of the most effective corrosion protective coatings for steel [1]. Recently, it was shown that the addition of alloying elements such as nickel (Ni) [2], chromium (Cr) [3], aluminum (Al) [4] and magnesium (Mg) [5] to the pure Zn increases its corrosion protection performance, considerably. The advantage of Mg over other elements can be described by its effectiveness even in a low alloying concentration [6]. The higher corrosion resistance of ZnMg coatings, as compared to the pure Zn, is related to the formation of a dense protective layer called “simonkolleite” by the addition of magnesium, which acts as a barrier to the corrosive media [7]. Different methods are commonly used to deposit pure or alloyed Zn coatings on steel substrates, such as hot-dip galvanizing (HDG) and electrodeposition [8]; however, some drawbacks occur, such as the inability of producing highly alloyed ZnMg coatings, depositing multilayered coatings, hydrogen embrittlement (especially for advanced high-strength steels), high temperature impact on the steel, high costs and environmental impact that can limit their applicability. Physical vapor deposition (PVD) can be considered as a favorable technique to replace the conventional methods, as it can be performed at much lower substrate temperatures (~250–300°C) and fulfills strict environmental regulations [9].



Although the addition of Mg to the Zn is beneficial for corrosion resistance, it reduces the adhesion of the coating to the steel substrate [10], [11]; however the effect of the Mg content of the ZnMg layer and also the relation between the thickness of the Zn interlayer and of the ZnMg top layer on the adhesion of ZnMg-Zn coatings are not yet fully understood. To fill this gap, a series of ZnMg-Zn bi-layered coatings with different Mg concentrations and also different thicknesses of the Zn and ZnMg layers were deposited on steel substrates, and then each was evaluated by both bending and scratch tests.

2 EXPERIMENTS

ZnMg-Zn bi-layered coatings (with different Mg concentrations, 0 to 14.1 wt.% Mg) and also different thicknesses of the Zn and ZnMg layers, were deposited on a low-carbon steel substrate (commonly called black plate steel) and a DP800 type of steel, using a thermal evaporation process. The chemical composition of the steel substrates is shown in Table 1.

Table 1: Chemical composition (wt.%) of DP800 and black plate steels.

Substrate	C	Si	Mn	P	S	Ni	Cr	Cu	Fe
DP800	0.153	0.386	1.487	0.013	0.007	0.018	0.02	0.015	Bal.
Black plate	0.04–0.08	0.03	0.18–0.35	0.02	0.03	0.08	0.08	0.08	Bal.

The vacuum chamber of the PVD machine is equipped with two crucibles containing pure Zn and a ZnMg alloy, respectively. The surface of the steel strip is pretreated by a plasma magnetron-based sputter unit, to remove any surface oxides. The evaporators use an induction coil system to melt and thermally evaporate the Zn-ZnMg source material. The metal vapor passes through a vapor distribution box and is deposited on the surface of the running steel strip. The ZnMg top layers are labelled as ZnMgX, with X indicating the Mg content in weight percent.

Grazing angle X-ray diffraction was used to analyze the phases present in the ZnMg layer. The incidence angle was set at 2° for all of the coatings, to ensure that the diffracted X-ray is only generated from the top layer, in order to discard the effect of the Zn interlayer. The cross-sections of the samples were mounted in an epoxy resin, ground by SiC paper, and finally polished up to 1 μm diamond particles in an ethanol lubricant. The microstructure of these coatings was evaluated using scanning electron microscope (SEM), a Philips XL30 ESEM.

A CSM Revetest scratch tester was used to quantify the adhesion strength of the ZnMg-Zn bi-layered coatings at the ZnMg/Zn interface. In this test, a diamond stylus (Rockwell C indenter with the tip radius of 200 μm) is moved along the coating with a progressively increasing load. The load at which the first visible failure (observing the pure Zn layer underneath) is recognized, is considered to be the critical load (L_C).

The maximum load and scratch length were considered as 20 N and 10 mm, respectively, for all bi-layered coatings. A minimum of 5 scratches were made and the average L_C was reported for each sample. BMW crash adhesion tests (BMW AA-M223) were also carried out, to study the adhesion performance of the coatings during bending load. This method is a standard adhesion test method, broadly used in industry to qualify the adhesion of galvanized coatings. Initially, a line of an adhesive (Betamate 1496V DOW Automotive Systems) at least 150 mm in length, 4–5 mm thick and at least 10 mm in width was applied to the surface of the coating. The samples were kept at 175°C for half an hour (30 minutes) to cure the adhesive. After cooling, the samples were quickly bent over a 90° angle. To pass the test, the adhesively bonded joint should fail in the adhesive, not in the coating/substrate interface. The BMW adhesion test was repeated three times for each sample. More information about this test can be found elsewhere [12].

3 RESULTS AND DISCUSSION

Fig. 1 shows the phase fraction of ZnMg coatings versus the Mg concentration, as determined by the grazing angle XRD. When the Mg content is low (<1.5 wt.% Mg), the top layer mostly consists of pure Zn. With an increase in the Mg content, the phase fraction of Zn decreases gradually, while the fraction of Mg_2Zn_{11} increases. The coating is composed of a mixture of Mg_2Zn_{11} and $MgZn_2$ at Mg concentrations that are higher than 6 wt.%. The phase fraction of $MgZn_2$ increases with further increases in Mg; and the ZnMg top layer coating is almost fully covered by this phase at ~14 wt.% Mg. Fig. 2 shows the cross-sectional SEM micrographs of the ZnMg-Zn bi-layer coatings, with different Mg concentrations. The thicknesses of the Zn interlayer and the ZnMg top layer for each coating are presented in Table 2. Microstructural studies also confirm the results as found by the XRD measurements.

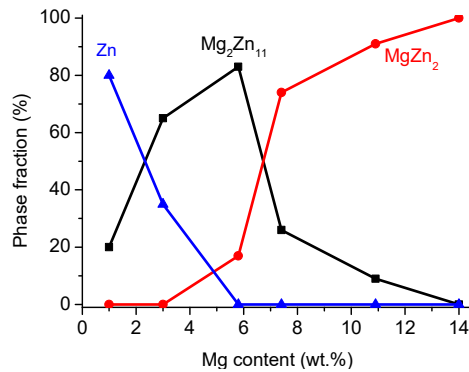


Figure 1: Phase fraction of ZnMg versus Mg content in the range of 1.5–14.1 wt.% Mg.

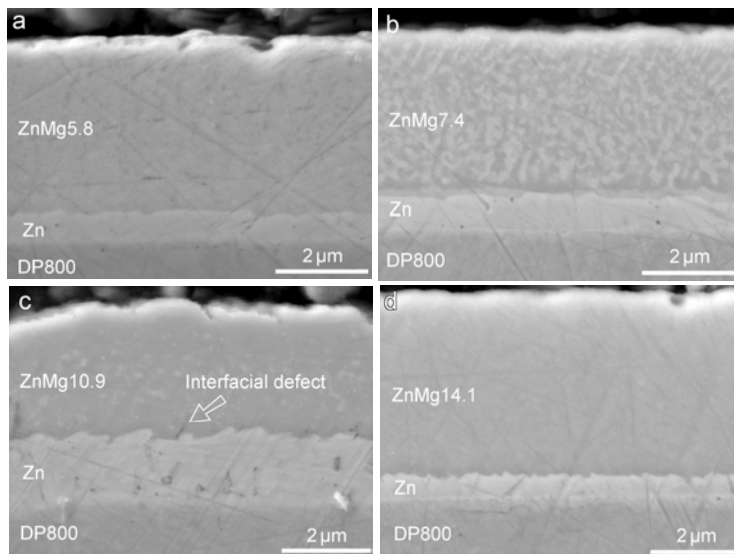


Figure 2: SEM micrographs showing cross sections of ZnMg-Zn bi-layered coatings with a ZnMg top layer, at the different Mg concentrations (wt.%): (a) 5.8; (b) 7.4; (c) 10.9; (d) 14.1.

Table 2: Adhesion strength of pure Zn and ZnMg-Zn bi-layer coatings containing different Mg contents measured using scratch test.

Coating	Thickness of Zn layer (μm)	Thickness of ZnMg layer (μm)	Critical load L_C (N)	Residual depth at L_C (μm)	Weight factor (ω)	Adhesion strength (MPa)	BMW adhesion test
Pure zinc	4.9	0	38.5 ± 1.5	-	-	171	pass
ZnMg5.8-Zn	0.7	3.9	18.1 ± 0.6	4.3	0.16	129	pass
ZnMg7.4-Zn	0.9	3.7	13.2 ± 0.7	3.3	0.27	103	pass
ZnMg10.9-Zn	1.6	3.1	9.3 ± 0.6	2.0	0.80	54	not pass
ZnMg14.1-Zn	0.6	4.4	8 ± 0.6	1.9	0.31	78	pass

Scratch tests were carried out to study the effect of the Mg concentration on the interfacial adhesion strength between the ZnMg and the Zn layer. Table 2 summarizes the critical load of delamination for each coating. It is worth mentioning that the overall thickness of all the coatings is in the same range, 4.6–5 μm . The critical load of the delamination for the pure Zn coating (38.5 N) is higher than that of all other ZnMg-Zn coatings. L_C decreases with increasing Mg concentration, reaching 18.1 N and 13.2 N, at 5.8 wt.% and 7.4 wt.% Mg, respectively. Further reduction of L_C is observed at even higher Mg content. The BMW crash adhesion test revealed that all of the coatings could pass the test, except the ZnMg10.9-Zn coating; however, the L_C of this coating is still higher than that of ZnMg14.1-Zn. Therefore, it can be concluded that L_C is not a suitable criterion to compare the adhesion of different ZnMg-Zn bi-layered coatings with different Mg concentrations and/or different layer thicknesses.

To find a proper way to quantify adhesion, the interfacial adhesion strength at the ZnMg/Zn interface was calculated using the modified Benjamin-Weaver model [13], as follows:

$$F = \frac{K a H}{\sqrt{R^2 - a^2}}, \quad (1)$$

where F is the adhesion strength (in MPa); K is constant; R is the radius of the indenter tip; H is considered as the hardness of the substrate; and a is the radius of the contact circle at L_C , as shown in eqn 2.

$$a = \left(\frac{L_C}{\pi H}\right)^{0.5}. \quad (2)$$

To consider the effect of both steel and zinc as the substrate for the ZnMg top layer, composite hardness was calculated, using a defined weight factor, as follows:

$$\omega = \frac{\text{Thickness of zinc interlayer}}{\text{Residual depth at } L_C}, \quad (3)$$

$$H_{\text{composite}} = \omega H_{\text{Zn}} + (1 - \omega) H_{\text{steel}}. \quad (4)$$

The adhesion strength of the PVD pure Zn on the steel substrate is 171 MPa, which is very comparable with the 180 MPa reported earlier for the adhesion of hot-dipped pure Zn onto steel [14]. The adhesion strength at the ZnMg/Zn interface decreases gradually with an increase in the Mg concentration, and reaches up to 78 MPa at 14.1 wt.% Mg.

The results of the interfacial adhesion strength obtained by the Scratch test follow the same trend; with the results of the BMW adhesion test and the ZnMg10.9-Zn coating failing

during the bending, which also showed the lowest adhesion strength among samples. Such low adhesion strength is related to the interfacial defects, which are present at the interface (Fig. 2(c)). It is also worth mentioning that the modified model can nicely reproduce the results of the BMW adhesion test for the ZnMg14.1-Zn coating, in contrast to only the L_C method. The ZnMg14.1-Zn coating, which pass the BMW adhesion test, shows a higher interfacial adhesion strength when compared to the ZnMg10.9-Zn coating.

The coatings that contain 5–7 wt.% Mg are apparently good candidates for practical applications which require simultaneously good adhesion and corrosion performance of the ZnMg coatings. Therefore, to study the effect of the thickness of the Zn interlayer on adhesion, we prepared a series of coatings with the same Mg concentration (~6.5 wt.% Mg) in the ZnMg top layer and different thicknesses of the Zn interlayer (0.2, 0.7 and 1.3 μm) (Fig. 3).

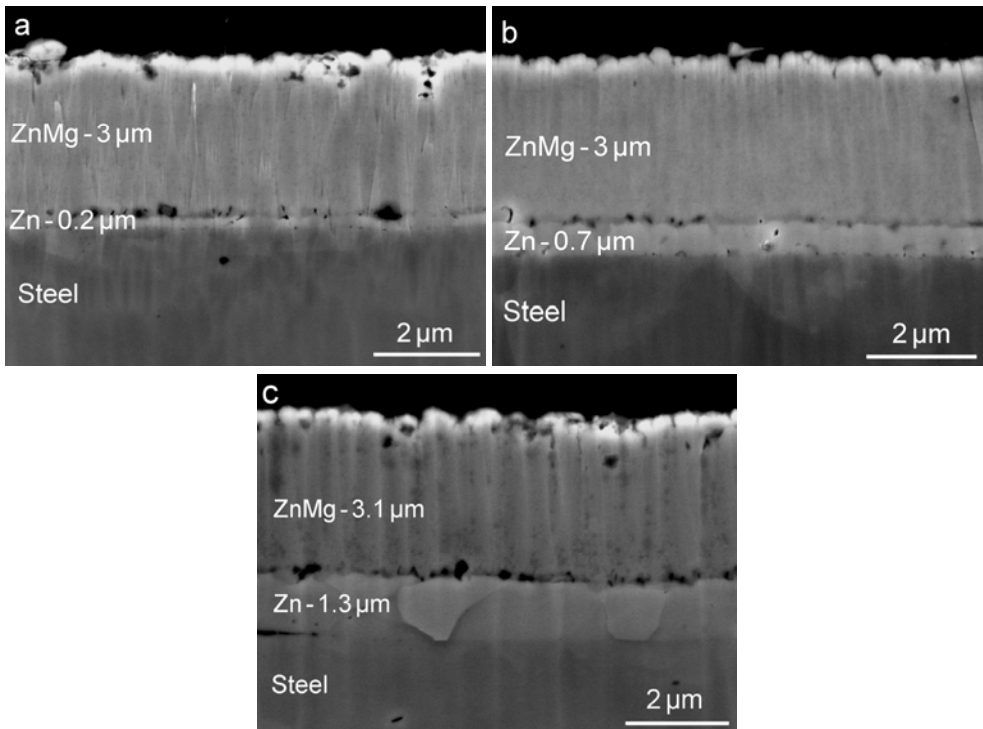


Figure 3: SEM micrographs of ZnMg6.5-Zn coatings with different thickness of the Zn interlayer: (a) 0.2 μm ; (b) 0.7 μm ; (c) 1.3 μm .

Fig. 4 shows the effect of the thickness of the Zn interlayer on the L_C (Fig. 4(a)) and the interfacial adhesion strength (Fig. 4(b)) of the ZnMg-Zn bi-layer coatings. The L_C increases with increases in the thickness of Zn from 11.6 to 13.25 N; however, the adhesion strength at the ZnMg/Zn interface is independent of the thickness, and is around 110 MPa for the ZnMg6.5-Zn coatings. It indicates that the Mg concentration plays the most dominant role in the interfacial adhesion strength, rather than the thickness. It should be noted that although the interfacial adhesion strength of all these coatings is the same, the coating with the lowest thickness of Zn failed in the BMW adhesion test, while

the others passed. It can be concluded that the adhesion performance of a substrate/coating system during bending does not only depend on the interfacial adhesion strength, but also the thickness of the Zn interlayer.

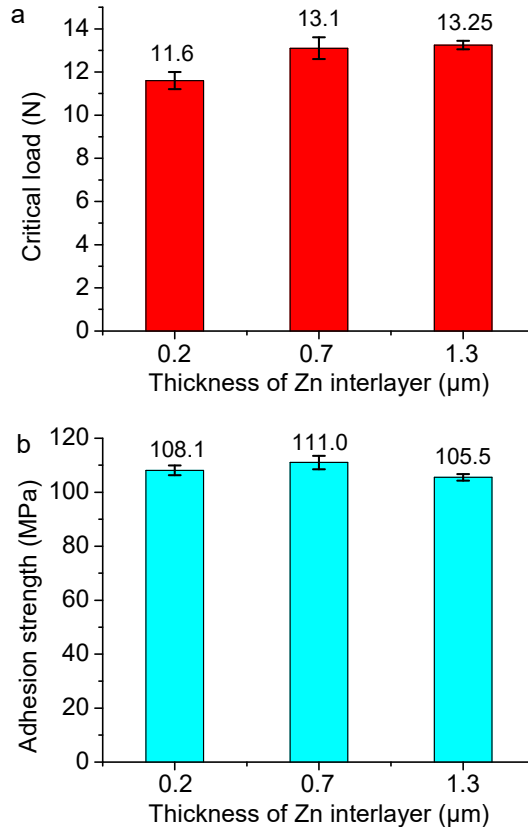


Figure 4: (a) Critical load of delamination and (b) interfacial adhesion strength of ZnMg6.5-Zn coatings, versus the thickness of the Zn interlayer.

It was shown previously that ZnMg-Zn bi-layered coatings with a sufficient thickness of the Zn interlayer and no interfacial defects between the Zn and ZnMg layer can pass the BMW adhesion test; however, it was also observed that the thickness of the ZnMg top layer can influence the adhesion performance of the coatings. The coatings fail in the BMW adhesion test when the thickness of ZnMg increases from a threshold level. Fig. 5(a) shows the cross-section SEM micrograph of a ZnMg14-Zn coating, with 6.8 μm thick top layer, which failed the BMW adhesion test. The SEM micrographs of the exposed side of the coating that remained on the substrate after the failure are shown in Fig. 5(b)–(d). The results of EDS analysis of different areas of the failed surface are shown in Table 3. Spot 1 consisted of 95.4 wt.% Zn and 4.6 wt.% Mg, while Spot 2 consisted of 84.5 wt.% Zn and 15.3 wt.% Mg. It should be mentioned that no sign of Fe is detected on the failed surface. These results clearly indicate that the ZnMg-Zn coatings with a relatively thick top layer experience failure in the BMW adhesion test, as cohesive brittle failure inside the ZnMg layer instead of adhesive failure at the interface.

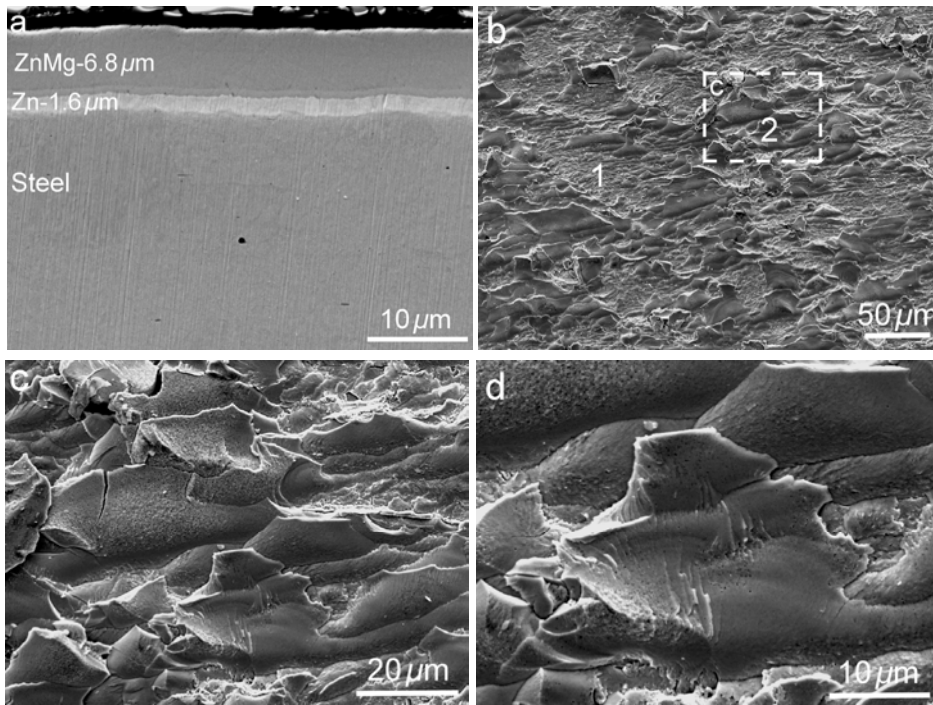


Figure 5: (a) SEM micrograph showing the cross section of ZnMg14-Zn coating containing 6.8 μm thick ZnMg top layer; (b)–(d) SEM micrographs of the exposed side of the coating which remains on the substrate after failure in the BMW crash adhesion test.

Table 3: Chemical composition of different points in Figure 5(b).

Location	Zn content (wt.%)	Mg content (wt.%)	Fe content (wt.%)
Spot 1	95.4	4.6	0
Spot 2	84.7	15.3	0

As a summary, it can be concluded that the adhesion performance of a ZnMg-Zn bi-layered coating during a bending test is a complex function of different parameters, such as the thickness of both the Zn and ZnMg layer, interfacial adhesion strength, and the interfacial defect density; as is schematically drawn in Fig. 6.

4 CONCLUSIONS

The effects of the Mg concentration and the thickness of Zn and ZnMg layers were studied on the adhesion of ZnMg-Zn bi-layered coatings, by the scratch and BMW crash adhesion tests. The novel findings are summarized as follows:

1. The critical load of the delamination is not a proper criterion through which to compare the adhesion of the ZnMg-Zn bi-layered coatings with different composition and/or thickness ratios.

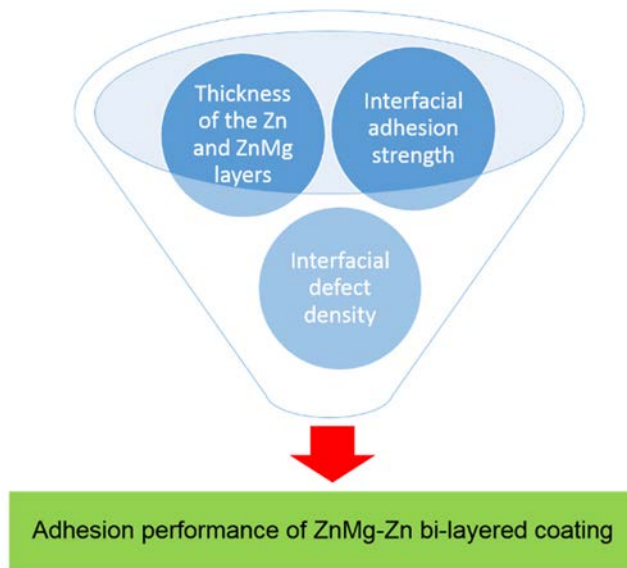


Figure 6: Parameters influencing the adhesion performance of ZnMg-Zn bi-layered coatings in the BMW crash adhesion test.

2. The Benjamin-Weaver model needs to be modified to be able to calculate the adhesion strength at the ZnMg/Zn interface by taking into account the L_C , thickness of the Zn interlayer, and the hardness of both substrate and interlayer.
3. The same trend is observed between the interfacial adhesion strength calculated by the scratch test and the BMW adhesion test, which is currently being used in industry for qualification of the adhesion.
4. The adhesion strength at the ZnMg/Zn interface depends on the Mg concentration of the top layer, but not on the thickness of the Zn interlayer. The interfacial adhesion strength decreases gradually, with increasing Mg concentrations.
5. The adhesion performance of a ZnMg-Zn bi-layered coating during a bending test is a complex function of different parameters, such as the thickness of the Zn and ZnMg layers, interfacial adhesion strength, and the defect density at the interface.

ACKNOWLEDGEMENTS

This research was carried out under project number S22.3.13513a within the framework of the Partnership Program of the Materials Innovation Institute M2i (www.m2i.nl) and the Technology Foundation TTW (www.stw.nl), which is part of the Netherlands Organization for Scientific Research (www.nwo.nl).

REFERENCES

- [1] Asgari, H., Toroghinejad, M.R. & Golozar, M.A., On texture, corrosion resistance and morphology of hot-dip galvanized zinc coatings. *Applied Surface Science*, **253**, pp. 6769–6777, 2007.
- [2] Rashmi, S., Elias, L. & Hedge, A.C., Multilayered Zn-Ni alloy coatings for better corrosion protection of mild steel. *Engineering Science Technology, an International Journal*, **20**, pp. 1227–1232, 2017.

- [3] Chakarova, V., Boiadjieva-Scherzer, T., Kovacheva, D., Kronberger, H. & Monev, M., Corrosion behaviour of electrodeposited Zn-Cr alloy coatings. *Corrosion Science*, **140**, pp. 73–78, 2018.
- [4] LeBozec, N., Thierry, D., Persson, D. & Stoullil, J., Atmospheric corrosion of zinc-aluminum alloyed coated steel in depleted carbon dioxide environments. *Journal of the Electrochemical Society*, **165**, C343–C353, 2018.
- [5] Dong, A. et al., Effect of Mg on the microstructure and corrosion resistance of the continuously hot-dip galvanizing Zn-Mg coating. *Materials*, **10**, p. 980, 2017.
- [6] Oh, M.S., Kim, S.H., Kim, J.S., Lee, J.W., Shon, J.H. & Jin, Y.S., Surface and cut-edge corrosion behavior of Zn-Mg-Al alloy-coated steel sheets as a function of the alloy coating microstructure. *Metals and Materials International*, **22**, pp. 26–33, 2016.
- [7] Pohl, K., Surface Chemistry and Corrosion Studies of Zn–Al and Zn–Mg–Al Alloy Coatings. PhD thesis, University of Paderborn, Germany, 2013.
- [8] Marder, A.R., The metallurgy of zinc-coated steel. *Progress in Materials Science*, **45**, pp. 191–271, 2000.
- [9] Navinsek, B., Panjan, P. & Milosev, I., PVD coatings as an environmentally clean alternative to electroplating and electroless processes. *Surface and Coatings Technology*, **116–119**, pp. 476–487, 1999.
- [10] La, J.H., Bae, K.T., Lee, S.Y. & Nam, K.H., A hybrid test method to evaluate the adhesion characteristics of soft coatings on steel substrates: Application to Zn-Mg coated steel. *Surface and Coatings Technology*, **307**, pp. 1100–1106, 2016.
- [11] Jung, W.S., Lee, C.W., Kim, T.Y. & De Cooman, B.C., Mg content dependence of EML-PVD Zn-Mg coating adhesion on steel strip. *Metallurgical and Materials Transactions A*, **47**, pp. 4594–4605, 2016.
- [12] Zoestbergen, E., Van de Langkruis, J., Maalman, T.F.J. & Batyrev, E., Influence of diffusion on the coating adhesion of zinc-magnesium thin films onto steel. *Surface and Coatings Technology*, **309**, pp. 904–910, 2017.
- [13] Sabooni, S., Galinmoghaddam, E., Ahmadi, M., Westerwaal, R.J., Van de Langkruis, J., Zoestbergen, E., De Hosson J.Th.M. & Pei, Y.T., Microstructure and adhesion strength quantification of PVD bi-layered ZnMg-Zn coatings on DP800 steel. *Surface and Coatings Technology*, **359**, 227–238, 2019.
- [14] Song, G.M., Sloof, W.G., Pei, Y.T. & De Hosson, J.T.M., Interface fracture behavior of zinc coatings on steel: Experiments and finite element calculations. *Surface Coating Technology*, **201**, pp. 4311–4316, 2006.

